Catalysis Today xxx (xxxx) xxx

Contents lists available at ScienceDirect

Catalysis Today

journal homepage: www.elsevier.com/locate/cattod

Peroxymonosulfate enhanced photoelectrocatalytic degradation of 17α-ethinyl estradiol

Rebecca Dhawle [a], Spyridon Giannakopoulos [a], Zacharias Frontistis [b,c], Dionissios Mantzavinos [a,*]

[a] Department of Chemical Engineering, University of Patras, 26500 Patras, Greece
[b] Department of Chemical Engineering, University of Western Macedonia, GR-50132 Kozani, Greece
[c] School of Sciences and Engineering, University of Nicosia, 2417 Nicosia, Cyprus

ARTICLE INFO

Keywords:
Photoelectrocatalysis
Estradiol
Peroxymonosulfate
Tungsten trioxide
Titanium dioxide
Synergy

ABSTRACT

This work aimed at the degradation of the synthetic estrogen 17α-ethinyl estradiol (EE2) via a combined photoelectrocatalysis (PEC) and peroxymonosulfate (PMS) process. Pristine and combined TiO_2/WO_3 photoanodes were fabricated and used in this work. The removal of 1 mg L^{-1} of EE2 increased from 47.9 % to 88.8 % in 60 min by adding 10 mg L^{-1} of PMS and an external bias of 1 V. EE2 was degraded in the presence of 0.05 M sodium sulfate as the electrolyte. The rate constant for the combined PEC-PMS process was 0.044 min^{-1} which was higher than the rate constant of light-activated PMS process (0.0053 min^{-1}) and PEC process (0.01 min^{-1}). The rate of EE2 degradation was increased with an increase in the voltage and PMS concentration. EE2 removal was decreased and reached 62.5 % and 48.5 % when 0.05 M NaCl or 0.05 M $NaClO_4$ was used respectively as the electrolyte, highlighting the crucial role of electrolytes in process efficiency. Both radical and non-radical mechanisms participated in the destruction of EE2, however the role of the photogenerated carriers was dominant. Ecotoxicity using *Vibrio fischeri* as an indicator was decreased, although not proportionately to the parent compound EE2 in the combined Solar/TiO_2/WO_3/PMS system.

1. Introduction

The increased consumption of pharmaceutical compounds across the globe has led to their accumulation in several water bodies. These compounds and their metabolites, excreted by humans and animals, make their way into different water sources. A total of 631 human and veterinary pharmaceuticals were detected in surface, ground, and drinking waters in 71 countries [1]. These active pharmaceutical ingredients present in water can induce mutagenicity, carcinogenicity, alteration in mental health, and physiological characteristics in living organisms [2]. Endocrine disrupting chemicals (EDCs) are highly potent compounds that could affect the hormonal functions of living organisms at concentrations as low as ng/L. These compounds alter the immune and reproductive systems and cause irreversible damage to human life and the environment [3]. 17α-ethinyl estradiol (EE2) is a synthetic estrogen that is widely used in the form of birth control pills. It is also one of the most detected hormones in municipal effluents. EE2 has detrimental effects on the embryonic development of organisms when tested in environmentally relevant concentrations [4]. The feminization of young male zebra fish (Danio rerio) into phenotypic females when exposed to concentrations as low as 100 ng L^{-1} of EE2 has been reported [4], among other embryonic development growth issues [5]. These studies indicate the potential toxicity of EE2 on the aquatic environment and, thus, on human health. The constant detection of such hormones in municipal effluents proves that they resist the conventional water treatment technologies used in treatment plants. Advanced oxidation processes have emerged as a solution to such persistent compounds. More specifically, photoelectrocatalysis (PEC) has proven effective in removing a wide range of micropollutants by the efficient use of both light and electrical energy while overcoming the major drawbacks such as (i) the recombination of photogenerated electron-hole pairs that occurs in a conventional photocatalytic process and (ii) the higher energy demand of an anodic oxidation process [6]. PEC processes necessitate the immobilization of a photocatalyst on an electrode surface, eliminating the need for catalyst separation and regeneration at the end of the process.

* Corresponding author.
E-mail address: mantzavinos@chemeng.upatras.gr (D. Mantzavinos).

https://doi.org/10.1016/j.cattod.2023.02.003
Received 6 September 2022; Received in revised form 30 January 2023; Accepted 3 February 2023
Available online 4 February 2023

Titanium dioxide (TiO_2), an n-type semiconductor ($E_{bg} = 3.2$ eV), is a widely used photocatalyst due to its high stability and low cost [7]. The use of TiO_2 for the removal of micropollutants in water matrices and other environmental applications is a widely explored domain. The activity of (TiO_2) results from the absorption of photons that occurs after irradiation leading to the formation of holes (h^+) [8]. These holes and OH radicals oxidize the organic pollutants on the surface [9]. The photocatalytic activity of TiO_2 occurs mainly in the ultraviolet spectra, which is a significant limitation. WO_3, on the other hand, is also an n-type semiconductor ($E_{bg} = 2.5$ eV) that is photoactive in the visible light spectrum. A combination of these two semiconducting materials would lead to an absorption shift into the visible range of the solar spectrum due to the relative positions of the conduction band and the valence band of the two materials. Consequently, the photoactivity of this combined photocatalyst would be enhanced due to a slower recombination rate of the photo-generated charge carriers [10].

Sulfate radical oxidation processes (SR-AOPs) have recently gained popularity due to their high oxidation potential (2.5–3.1 V). Sulfate radicals can be generated following the activation of persulfate and monosulfate compounds through different methods such as light irradiation [11,12], heat [13,14], ultrasound [15], and catalytic materials derived from carbon [16] and metals [17]. With novel and cheaper activation methods, the generation of sulfate radicals has become non-complex and economical.

In this work, the photoelectrochemical removal of the synthetic estrogen EE2 has been enhanced using peroxymonosulfate on a hybrid TiO_2/WO_3 photoanode and simulated solar irradiation. The effect of PMS addition, electrolytes, and the applied potential on the removal has also been studied. The contribution of both radical and non-radical mechanisms was assessed, while monitoring of the ecotoxicity provided valuable insights for evaluating the environmental impact of the process.

2. Material and methods

2.1. Chemicals

All chemicals were purchased from Sigma-Aldrich and used as received. Fluorine-doped tin oxide (8 Ω sq^{-1}) was purchased from Pilkington, USA. Ultrapure water was used for all experimental work. EE2 stock was prepared in absolute ethanol to ensure complete solubility.

2.2. Preparation of Photoanodes

The TiO_2 precursor solution was prepared by mixing 1.8 mL of titanium isopropoxide with 19 mL ethanol, 3.4 mL glacial acetic acid, and 3.5 g of Triton-X until a transparent viscous solution was obtained. For the WO_3 precursor solution, 0.4 g of high-purity tungsten powder (avg. particle size 10 μm) was dissolved in 3 mL of 30 % peroxide solution and sonicated for 3 h until a clear solution was obtained. Excess of peroxide was catalytically decomposed using a platinum wire at 4 °C overnight and later mixed with 3 mL of ethanol and 0.3 g of Triton-X. The FTO glass was cut to the required dimensions and washed with soap. It was then sonicated with acetone, ethanol, and water and dried at 70 °C. The FTO glass was dipped in the TiO_2 precursor and dried at 80 °C for 20 min and then sintered at 550 °C at 20 °C min^{-1}. The procedure was repeated to ensure a uniform layer. The WO_3 solution was deposited on the TiO_2 layer by spin coating at 3000 rpm. It was sintered at 500 °C for 10 min. This procedure was repeated three times until a pale-yellow color was observed. The active electrode area was 2.5 cm × 2.5 cm.

2.3. Experimental setup

A rectangular quartz beaker was used as an undivided electrochemical reactor. Sixty mL of the electrolyte containing 1 mg L^{-1} of EE2, and 10 mg L^{-1} of PMS was introduced into the reactor. The as-prepared TiO_2/WO_3 electrode was suspended in the reactor and irradiated using a 100 W xenon ozone-free solar simulator (Oriel, model LCS-100). A platinum wire was used as a counter electrode with an Ag/AgCl electrode as a reference. The solution was placed under constant stirring with the help of a magnetic stirrer. At regular time intervals, 1.2 mL of the samples were drawn from the reactor, quenched with 0.3 mL of methanol, and filtered before analysis.

2.4. Analytical methods

Electrochemical electrode characterization was carried out using a three-electrode system containing 60 mL of 0.05 M Na_2SO_4 solution at inherent pH. A platinum electrode was used as a counter and an Ag/AgCl electrode as a reference. The voltammograms were recorded for values between − 1 and 1.5 V at a scanning rate of 20 mV s^{-1}. All the current-voltage measurements were made with an Autolab Potentiostat PGSTAT128N (Utrecht, The Netherlands).

EE2 concentrations were monitored using high-performance liquid chromatography. The mobile phase consisted of 60:40 acetonitrile: water eluted isocratically at 45 °C. Kinetex XB-C18 100 A column (2.6 μm, 2.1 mm × 50 mm) was used to achieve separation. EE2 was detected at $\lambda = 235$ nm using a photodiode array detector (Waters 2996 PDA). The toxicity was estimated using the luminescent marine bacteria *V. fischeri*. More details can be found in a previous study [18].

3. Results and discussion

3.1. Electrochemical characterization of the photoanode

Fig. 1 shows the voltammetric behavior of the photoanode in a 0.05 M Na_2SO_4 solution with and without irradiation. 10 voltammetric cycles were repeated within a potential range of − 1 to 1.5 V, and identical profiles for the voltammogram were obtained, indicating the high stability of the photoanode.

The obtained profile for the CV depicted peaks corresponding to the redox reactions occurring at the anode and the cathode. The graph clearly shows the photoelectroactivity of the synthesized electrodes. A maximum current density of 2.21 mA cm^{-2} was obtained at an applied potential of 1.5 V, almost 20 times higher than the current density obtained without irradiation. This maximum value obtained is also higher than previously reported for pristine TiO_2 films [19], showing that the TiO_2/WO_3 films show better photoelectrochemical behavior.

The effectiveness of charge carriers' recombination, migration, and transfer was examined for comprehending the mechanism underlying

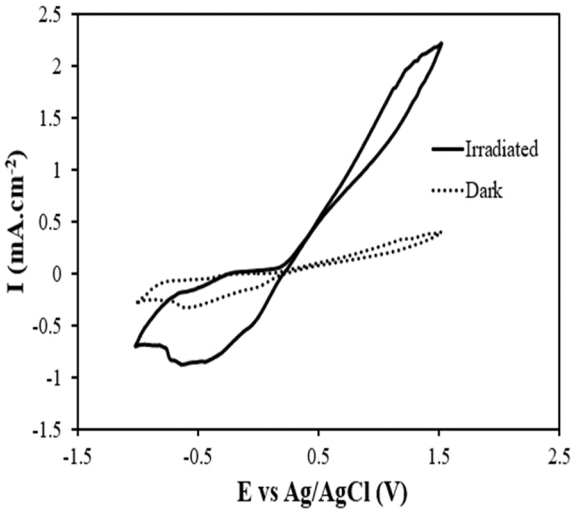

Fig. 1. Cyclic voltammetry of the fabricated TiO_2/WO_3 photoanode.

the increased photocatalytic activity of the as-prepared TiO_2/WO_3. Therefore, photoelectrochemical tests were conducted to investigate the excitation and transfer of the photogenerated charge carriers. Higher charge carrier separation and photocurrent are correlated with higher photocatalytic activity [20–22]. More specifically, the transient photocurrent response of the prepared photocatalytic samples was evaluated in Na_2SO_4 aqueous solutions under simulated solar irradiation with many cycles of 50 s interval light on or off.

According to Fig. 2(a), when the light source was turned on, the photocurrent value of the TiO_2/WO_3 surged abruptly to a high current level before falling back to its original value. When the light was switched on again, it also returned to a consistent value. Contrarily, bare TiO_2 showed no discernible photocurrent response, while the WO_3 maximum photocurrent value failed to surpass the value of the composite photocatalyst.

The current/photocurrent density curves under dark/light are displayed in Fig. 2(b), (c). Since both WO_3 and TiO_2 are n-type semiconductors, the photocurrents grew as the applied anodic potential rose, exhibiting a typical n-type semiconductor behavior. The photogenerated current density of WO_3 was relatively lower, indicating a short lifetime and limited mobility of the photoproduced carriers. On the other hand, TiO_2 did not exhibit any discernible photocurrent response. When exposed to simulated solar irradiation, TiO_2/WO_3 had a significantly larger photocurrent density than the other samples. These outcomes confirmed that, when exposed to light, TiO_2/WO_3 had a much greater separation efficiency of the photogenerated electron-hole pairs [20].

Additionally, compared to bare WO_3, the photocurrent onset potential of TiO_2/WO_3 was negatively shifted to lower potential values (vs. Ag/AgCl). In general, the photocurrent onset potential shows the flat band potential of the electrode; by coupling with WO_3, whose flat band potential is less negative than that of TiO_2, the flat band potential of TiO_2 was altered to a more negative potential.

In a previous work, Castro et al. [20] examined the charge transfer mechanism of WO_3/TIO_2 heterojunction for hydrogen production using photoelectrochemistry. The authors observed a significant increase in the photocurrent in the presence of sacrificial agents acting as hole scavengers for the WO_3/TIO_2 film compared to WO_3.

The researchers used a Mott-Schottky plot to calculate a potential difference equal to 1.08 V between WO_3 and TiO_2 that facilitates the charge injection from one semiconductor to another. According to the proposed mechanism, when WO_3 is illuminated, the photogenerated holes from WO_3 can be easily diffused to TiO_2 due to appropriate work function and potential difference. Conversely, due to thermodynamic restrictions, the WO_3 photogenerated electrons are not allowed to be injected into the TiO_2 conduction band. Thus, the separation of the photoinduced species was increased, and therefore, the photoelectrochemical efficiency of the system was enhanced.

Fig. 2(d) shows the amperometric curves at 0.5 V, under periodically interrupted light irradiation, with or without the oxidizing agent. More specifically, PMS addition to the photoelectrochemical reactor causes the rapid reduction of the generated photocurrent, which does not exceed 10 μA cm^{-2}. This evolution indicates the intense action of PMS as an electron acceptor, which is activated towards the formation of sulfate radicals, whose existence is confirmed by kinetic experiments with radical scavengers. The fact that the oxidant acts as a photoelectron trap contributes to the lower electron availability that end up at the cathode and the produced photocurrent decrease; on the contrary, the number of photoproduced holes that are available for EE2 oxidation increases due to the weakening of the e-/h+ recombination rate. [23].

3.2. Effect of PMS

Initially, the photoelectrochemical decomposition of 0.5 mg L^{-1} of EE2 was examined using the fabricated TiO_2/WO_3 electrodes with an applied potential of 1 V (vs. Ag/AgCl) in the presence of 0.05 M Na_2SO_4 at the inherent pH of the solution; 47.9 % removal of EE2 was recorded

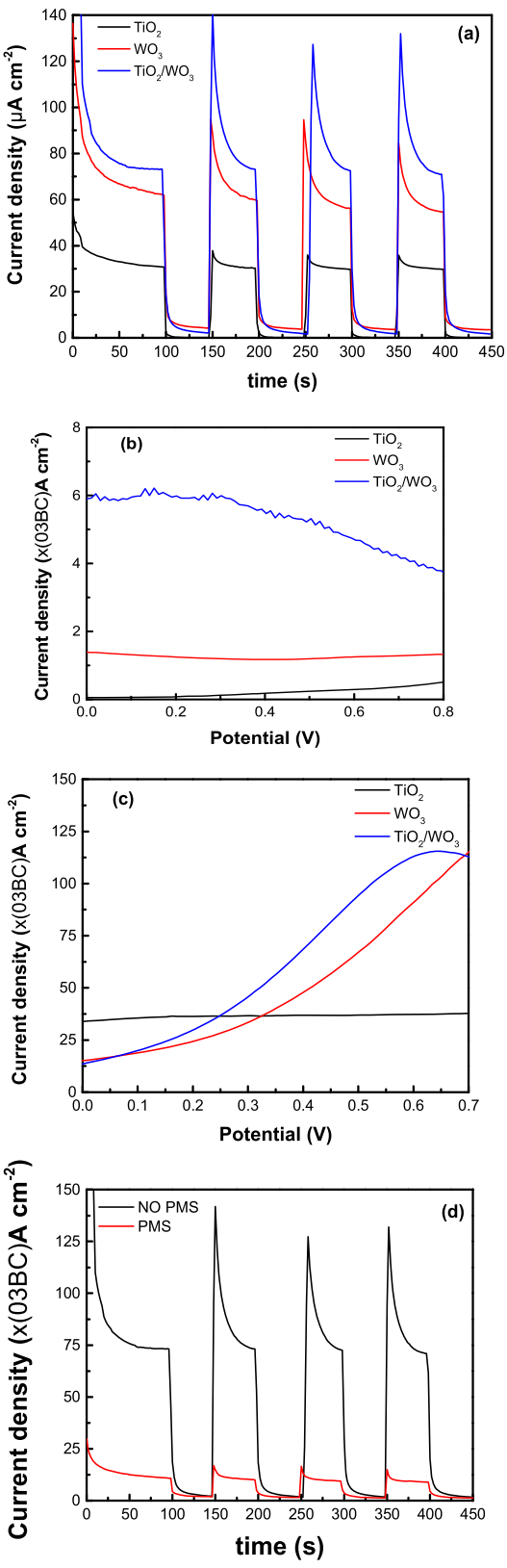

Fig. 2. (a) Amperometric I–t curves of the three electrodes at an applied potential of 0.5 V under light irradiation with 50 s light on/off cycles; (b) LSV curves under dark; (c) LSV curves under light; (d) Amperometric I–t curves of WO_3/TiO_2 at an applied potential of 0.5 V under light irradiation with 50 s light on/off cycles in the presence of PMS.

within 60 min and the apparent kinetic constant, k_{app}, for the PEC removal was found to be 0.01 min^{-1}. On adding 10 mg L^{-1} of PMS under the same experimental conditions, the removal efficiency of EE2 increased to 88.8 % with a k_{app} value of 0.042 min^{-1}.

Additional experiments were performed to evaluate the effects of individual processes. The removal of EE2 using different processes is shown in Fig. 3(a). Removal of 30.3 %, 2.7 %, 21.8 % and 25.9 % were obtained for solar-activated PMS, photocatalysis, electrochemical oxidation, and photocatalysis combined with PMS, respectively, as shown in Fig. 3(b). Using PMS along with PEC process increased the removal efficiency by almost two times. The synergistic effects of a combined process can be evaluated using the synergy index (S) using the following equation [24]:

$$S = \frac{k_{combined} - \sum_{i}^{n} k_i}{k_{combined}} \quad (1)$$

If $S > 0$, the combined process demonstrates synergistic effects, otherwise the process is either competitive ($S < 0$) or cumulative ($S = 0$). Replacing the values of rate constants for the combined process ($k_{PEC:PMS}$) and individual solar-activated PMS (k_{SolPMS}) and PEC (k_{PEC}) processes in equation (1), a synergy degree of 63.5 % was observed.

The effect of the PMS concentration is shown in Fig. 3(c). The decrease in the PMS concentration led to slower EE2 removal. 49.8 % and 27.9 % of EE2 was removed with 5 mg L^{-1} and 2.5 mg L^{-1} of PMS, which is almost 1.7 and 3 times lower than the removal of 88.8 % with

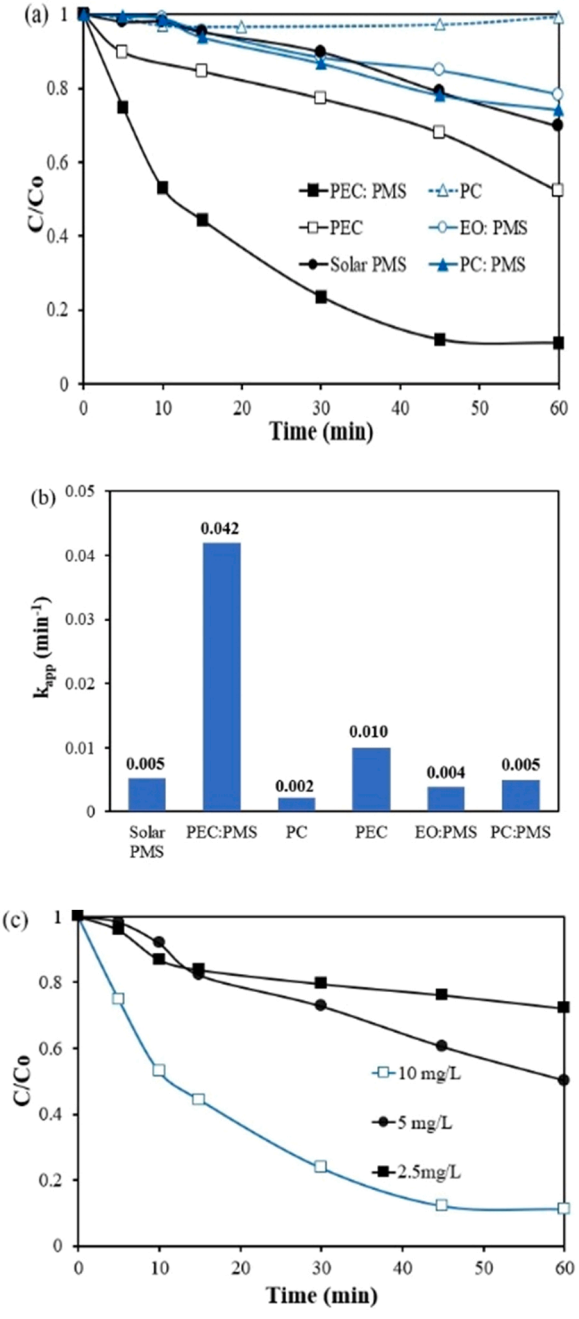

Fig. 3. Effect of PMS on the photoelectrochemical degradation of EE2. (a) Removal of 1 mg L^{-1} EE2 using different processes; (b) k_{app} for the removal of 1 mg L^{-1} EE2; (c) Effect of PMS concentration; EE2 = 1 mg L^{-1}; PMS = 10 mg L^{-1}; Na_2SO_4 = 0.05 M; 1 V.

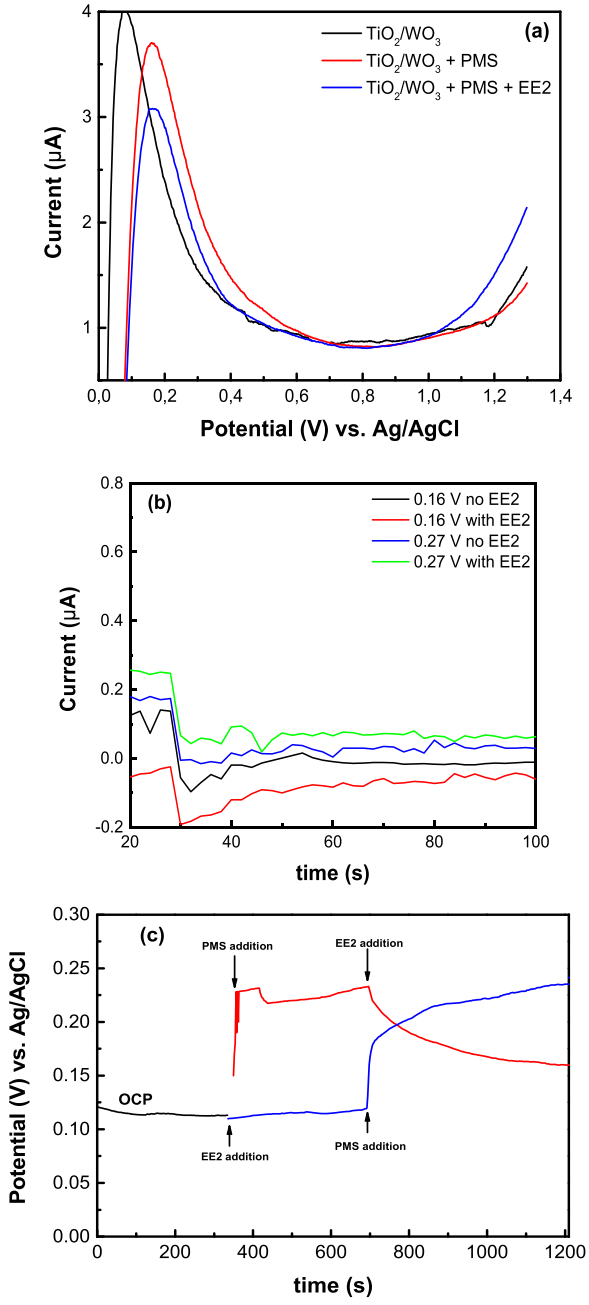

Fig. 4. (a): LSV curves in the absence of light under different conditions; (b) Amperometric I–t curves under different applied potentials in the dark; (c) open circuit potential curves with the presence of 0.1 Na_2SO_4 before and after adding 10 mg L^{-1} PMS or 1 mg L^{-1} EE2 at inherent pH in the dark.

10 mg L^{-1} of PMS respectively. Lowering the PMS concentration reduces the number of sulfate radicals, resulting in poor removal of EE2. Such trends for the effect of PMS concentration were observed in other studies [25,26]. Therefore, adding PMS positively affects the PEC process by generating a higher number of radicals for organic removal. However, an excessive increase in PMS concentration might not be favorable due to the formation of other undesirable radicals leading to a scavenging effect [27].

3.3. Radical and non-radical mechanisms

An interesting characteristic of persulfate-induced oxidation is that emerging contaminants can be degraded using either a radical or a non-radical mechanism [28].

Under this perspective, the electron transfer mechanism in the TiO_2/WO_3/PMS system was further explored using linear sweep voltammetry (LSV) measurement to understand better the non-radical-based PMS activation process in the absence of light. The electrochemical current provided to the working electrode allowed for the determination of the electron transfer by adding PMS and EE2. An interaction between PMS and the photocatalyst, as well as the electron rearrangement that results in the formation of metastable PMS, are shown in Fig. 2(a). The current formed and flowed through TiO_2/WO_3 with the presence of EE2 indicates that the photocatalyst acts as a bridge to enhance electron transfer from the EE2 molecule to the metastable PMS. This was particularly striking because the subsequent infusion of EE2, which led to additional current enhancement, implied a rapid transfer of electrons in the TiO_2/WO_3/PMS/EE2 system.

An assumed non-radical catalytic mechanism for the oxidation of EE2 in the TiO_2/WO_3/PMS system is based on the abovementioned investigations. A simple oxidation-reduction reaction occurred between the contaminant as an electron donor and the metastable PMS as an electron acceptor under the influence of TiO_2/WO_3 after the PMS molecules adsorbed on the photocatalyst were stimulated to the metastable condition. Then, to accomplish the goal of EE2 conversion, the metastable PMS molecules extract electrons from EE2 molecules by TiO_2/WO_3.

In order to investigate in-depth, the existence of a mechanism for the direct oxidation of EE2 by the photocatalyst in the absence of radiation, amperometry experiments were carried out with and without oxidant according to Fig. 4. More specifically, TiO_2/WO_3 served as the anode electrode, a platinum wire as the cathode electrode, and Ag/AgCl as the reference electrode in the presence of 0.05 M Na_2SO_4.

Then the open circuit potential (OCP) was recorded, corresponding to 0.16 V vs. Ag/AgCl, and applied to record the produced current. The same experiment was conducted in the presence of EE2, where an increase in the negative current was found, indicating an improvement in charge mobility without, however, confirming the direct oxidation of the substance, i.e., without the mediation of active oxidizing species, as a depletion in the current would be expected since EE2 acts as an electron donor. Therefore, the redox potential of the photocatalyst is expected to be lower than the oxidation potential of EE2 under inherent pH (pH = 6.1).

Correspondingly, OCP was noted in the presence of 10 mg L^{-1} PMS, which was found to be higher, equal to 0.27 V vs. Ag/AgCl, essentially reflecting the fact that the oxidant acts as an electron acceptor. Then, the current was recorded as a function of time. The addition of pollutants contributed to a partial increment in the current, due to easier electron transfer from the formed TiO_2/WO_3/PMS/EE2 complex, as well as direct electron detachment from the TiO_2/WO_3/PMS system to the adsorbed oxidant molecule through the photocatalytic surface. In addition, in the case of semiconductors, due to their low conductivity compared to bare metals, the electrons could be directly transferred from EE2 to PMS without the solid catalytic surface. [28].

To investigate in depth the possible existence of a non-radical mechanism for EE2 oxidation, additional electrochemical voltammetry experiments were carried out in the absence of radiation and under galvanostatic current, corresponding to the open circuit potential (OCP = 0.135 V vs. Ag/AgCl) and the results are shown in Fig. 4(c) [29]. In the first phase, 10 mg L^{-1} PMS were added to the reactor, leading to a potential increment to 0.23 V vs. Ag/AgCl; this indicates that the oxidant acts as an electron acceptor hindering the uninterrupted charge flow through the external circuit and, consequently, resulting in the electric force rise to keep the current constant. Then, 1 mg L^{-1} EE2 was introduced into the solution causing the potential reduction, which may be attributed to the direct oxidation of the organic by the formed metastable TiO_2/WO_3 *PMS complexes; this pathway can improve the flow of electrons from EE2 to the catalytic surface and finally to the external circuit and requires the applied voltage abatement to keep the current constant.

On the contrary, when the organic was added first to the electrochemical cell, the voltage remained unchanged, showing that it is not oxidized by the photocatalyst in the absence of oxidant and light. When PMS was also added, the potential intensification again expresses the strong electron attraction of the adsorbed oxidant on the TiO_2/WO_3 surface stimulating the charge flow and conductivity of the material.

Therefore, the non-radical mechanism could be described from Eqs. (2)–(5), where TiO_2/WO_3 $_{ox}$, being the oxidized form of TiO_2/WO_3, could be a defect/impurity on the catalyst lattice or a photoproduced hole in the presence of irradiation.

$$TiO_2/WO_3 + HSO_5^- \rightarrow [TiO_2/WO_3 - HSO_5^-] \quad (2)$$

$$[TiO_2/WO_3 - HSO_5^-] \xrightarrow{\text{e−from TiO2/WO3.to PMS}} TiO_2/WO_{3ox} + SO_4^{2-} + OH^- \quad (3)$$

$$EE2 + \frac{TiO_2}{WO_{3ox}} \xrightarrow{\text{e−fromEE2.to}\frac{TiO_2}{WO_3}} \frac{TiO_2}{WO_3} + EE2_{ox} \quad (4)$$

$$EE2 + [TiO_2/WO_3 - HSO_5^-] \xrightarrow{\text{e − from EE2.to PMS}} EE2_{ox} + TiO_2/WO_3 + SO_4^{2-} + OH^- \quad (5)$$

On the other hand, the photoinduced system is capable of oxidizing via the electrogenerated holes and the produced reactive species, mainly hydroxyl and sulfate radicals. To further investigate the effect of the different reactive species in the decomposition of EE2, additional experiments were performed in the presence of scavengers. More specific EDTA was used for scavenging the photoproduced holes, tert-butanol

scavenged mainly hydroxyl radicals, while methanol scavenged both hydroxyl and sulfate radicals.

The decomposition of EE2 after 90 min decreased to 55 % in the presence of tert-butanol and 38 % in the presence of methanol. At the same time, the process was almost inhibited since only 17 % reduction was observed when EDTA was added, highlighting the dominant role of the photogenerated carriers.

Furthermore, for the PEC experiments performed in the absence of PMS, EE2 decomposition was 8 %, 22 % and 18 % in the presence of EDTA, methanol, and tert-butanol respectively, confirming again the crucial role of the photogenerated holes.

Therefore, the radical mechanism can be described as follows:

$$TIO_2/WO_3 \xrightarrow{hv} h^+ + e^- \quad (6)$$

$$HSO_5^- + e_{CB}^- \rightarrow SO_4^{\bullet -} + OH^- \quad (7)$$

$$HSO_5^- + h_{VB}^+ \rightarrow SO_5^{\bullet -} + H^+ \quad (8)$$

$$SO_5^{\bullet -} + SO_5^{\bullet -} \rightarrow 2SO_4^{\bullet -} + O_2 \quad (9)$$

$$H_2O + h_{VB}^+ \rightarrow {}^{\bullet}OH + H^+ \quad (10)$$

$$EE2 + SO_4^{\bullet -} \rightarrow CO_2 + H_2O + \text{intermediates} \quad (11)$$

$$EE2 + h^+ \rightarrow CO_2 + H_2O + \text{intermediates} \quad (12)$$

$$EE2 + {}^{\bullet}OH \rightarrow CO_2 + H_2O + \text{intermediates} \quad (13)$$

3.4. Effect of electrolytes

Electrolytes play an important role in the removal process and influence the generated by-products. Experiments were performed with 0.05 M NaCl and 0.05 M $NaClO_4$. The effect of electrolyte on EE2 removal is shown in Fig. 5(a). As seen, the presence of chloride in the PEC system inhibited the removal of EE2. Many studies have reported an enhanced effect of chloride on removal due to the side reactions leading to the formation of active chlorine species [30,31]. The inhibitory effects of chloride could, however, occur due to (i) the blockage of active sites on the surface of the photoanode [32] and/or (ii) chloride either acting as scavenger for hydroxyl radicals or as recombination center for the charge carriers [33]. Similar results have also been reported in a study evaluating the role of chloride in the PEC removal of diethyl phthalate from water [34]. In general, $NaClO_4$ is considered an inert electrolyte. However, in the present study, the use of $NaClO_4$ resulted in a significant decrease in the destruction of EE2. The observed efficiency reduction may be attributed to competition for the catalytic surface and reaction with hydroxyl radicals, as well as the detrimental effect of the highly acidic pH of the solution [35].

The detrimental effect of the electrolyte concentration is shown in Fig. 5(b). 60.4 % and 53.8 % of EE2 is removed increasing the concentration of Na_2SO_4 to 0.1 M and 0.5 M, respectively. The high number of sulfate radicals favors the formation of persulfate, which has a lower standard redox potential than $SO^{\bullet -}$ and $^{\bullet}OH$ radicals. This explains the lower removal of EE2 at higher concentrations of Na_2SO_4. Similar results have been reported by Chen et al. [36], who studied the electrochemical activation of sulfate over a BDD anode and titanium cathode for the decomposition of the 2,4-dichlorophenol. The authors observed that the efficiency of the combined process increased with the electrolyte concentration up to an optimum level (0.2 M) and then decreased, exhibiting a volcano-type behavior.

3.5. Effect of applied potential

Another key factor in the PEC process is the applied potential. Experiments were performed at applied potentials of 0.25 V, 0.5 V, and 1 V and the results are shown in Fig. 6. The higher removal (88.8 %) was obtained at an applied potential of 1 V, while the lower (51.3 %) at 0.25 V. The applied potential prevents the recombination of charges by driving the photo-generated electrons to the cathode and away from the surface of the photoanode, thus allowing the holes to oxidize the organics present in the system. Increasing the potential beyond 1 V could reduce the current efficiency of the photoanode and not enhance the removal of EE2 any further due to the oxygen evolution that occurs at 1.5 V as demonstrated in Fig. 1. Therefore, no significant increase in the EE2 removal is expected in increasing the applied potential beyond 1 V.

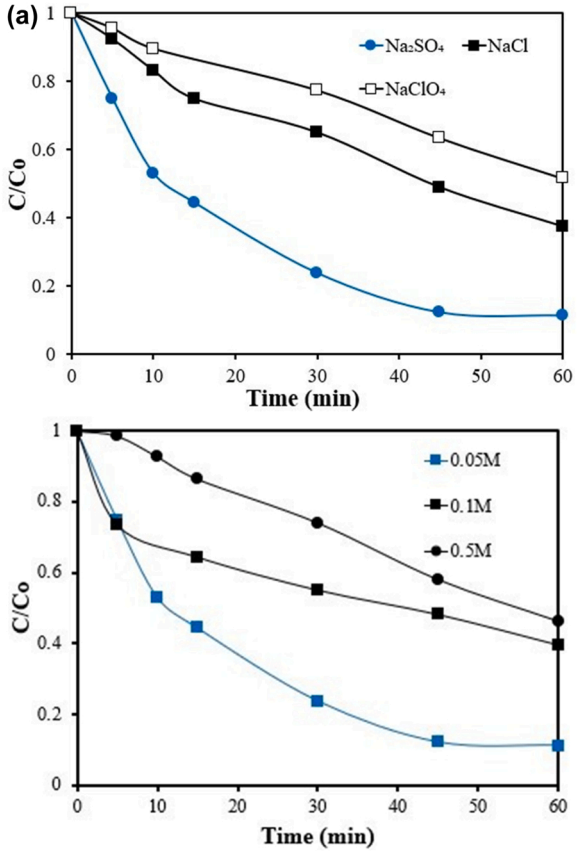

Fig. 5. (a) Effect of 0.05 M of various electrolytes on the removal of EE2; (b) Effect of Na_2SO_4 concentration. EE2 = 1 mg L^{-1}; PMS = 10 mg L^{-1}; 1 V.

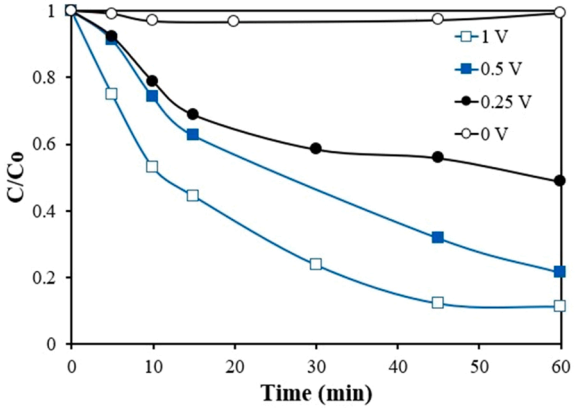

Fig. 6. Effect of the applied potential on the removal of 1 mg L^{-1} EE2. PMS = 10 mg L^{-1}; Na_2SO_4 = 0.05 M.

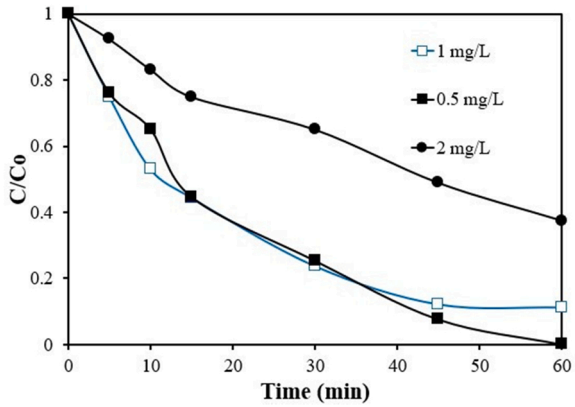

Fig. 7. Effect of initial EE2 concentration on its removal. PMS = 10 mg L^{-1}; Na_2SO_4 = 0.05 M; 1 V.

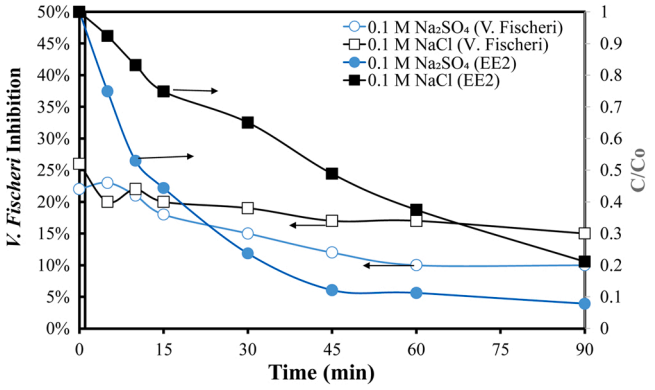

Fig. 8. Inhibition of *V. fischeri* and associated EE2 removal. Na_2SO_4 or NaCl = 0.05 M; EE2 = 1 mg L^{-1}; PMS = 10 mg L^{-1}; 1 V.

3.6. Effect of EE2 concentration

The effect of initial EE2 concentration on its removal is shown in Fig. 7. It can be seen that an increase in EE2 concentration reduces the removal efficiency. This behavior has been observed in various advanced oxidation processes and is due to (i) mass transfer limitations, and/or (ii) limitations on the production of reactive species. Higher concentrations of organic compound occupy more active sites, and this may prevent the light from reaching the surface of the photocatalytic films [37]. In addition, increasing the concentration of EE2 under constant experimental conditions increases the ratio of organics to the available reactive species. Therefore, the radicals available for EE2 are insufficient. Thus, the generation of the reactive species can be considered a limiting factor [38].

3.7. Toxicity

Although advanced oxidation processes could conceptually lead to mineralization of the target contaminants, this usually is not the case since very intensive conditions or prolonged treatment times are required. Therefore, the resulting stream often contains a mixture of oxidation by-products. In this respect, it is crucial to investigate the toxicity of the treated solution. This was done using the bacterium *V. fischeri* as an indicator, and the results are depicted in Fig. 8. As seen, the decrease in toxicity is not proportional to the elimination of EE2, thus implying that certain by-products formed may also induce toxicity to V. *fischeri*; this said, the starting value of the untreated solution is rather low, i.e., 20–25 %. Notably, the experiment performed with NaCl as the electrolyte was not detrimental to the indicator, thus indicating that toxic organochlorinated by-products are not formed at considerable concentrations at the conditions in question. However, these results must be viewed with caution since they are limited to a specific indicator and experimental conditions. In future work, research is needed for an integrated assessment of toxicity using specific tests regarding the estrogenicity of the treated solution.

4. Conclusions

The use of relatively low quantities of PMS (10 mg L^{-1}) in a PEC system showed promising results in removing 88.8 % of the steroid EE2. Increasing PMS concentration and applied potential positively affected EE2 removal. However, an increased electrolyte concentration or the presence of chloride had detrimental effects on process efficiency.

The fabricated TiO_2/WO_3 electrodes showed better electrochemical behavior and higher photoelectrochemical response than pristine TiO_2 photoanodes. According to the electrochemical measurements and experiments that were conducted using scavengers of the reactive species, both radical and non-radical mechanisms occurred; however, the role of photogenerated holes and electrons was vital and the driving force for the EE2 decomposition. At the same time, both hydroxyl and sulfate radicals participated in the degradation.

Although the toxicity of the treated solution to *V. fischeri* was decreased, the trend did not follow the removal of EE2, implying the formation of some toxic intermediates. The proposed PEC/PMS system needs to be further evaluated to determine its feasibility for treating complex water matrices, and an integrated toxicity assessment is needed to this direction.

CRediT authorship contribution statement

Rebecca Dhawle: Investigation, Validation, Writing – original draft. **Spyridon Giannakopoulos:** Investigation, Validation, Writing – review & editing. **Zacharias Frontistis:** Conceptualization, Methodology, Investigation, Writing – review & editing. **Dionissios Mantzavinos:** Conceptualization, Resources, Writing – review & editing, Supervision, Funding acquisition.

Declaration of Competing Interest

The authors declare that they have no known competing financial interests or personal relationships that could have appeared to influence the work reported in this paper.

Data Availability

No data was used for the research described in the article.

Acknowledgements

This project has received funding from the European Union's EU Framework Programme for Research and Innovation Horizon 2020 under Grant Agreement No 861369. (innoveox.eu).

References

[1] T. aus der Beek, F.-A. Weber, A. Bergmann, S. Hickmann, I. Ebert, A. Hein, A. Küster, Pharmaceuticals in the environment–global occurrences and perspectives, Environ. Toxicol. Chem. 35 (2016). ⟨https://10.1002/etc.3339⟩.
[2] OECD, Pharmaceutical residues in freshwater: Hazards and policy responses. ⟨https://10.1787/c936f42d-en⟩.
[3] K.X. Vargas-Berrones, L.A. Bernal-Jácome, L.D. de León- Martínez, R. Flores-Ramírez, Emerging pollutants (EPs) in Latin América: a critical review of under-studied EPs, case of study- Nonylphenol, Sci. Total Environ. 726 (2020), 138493, https://doi.org/10.1016/j.scitotenv.2020.138493.
[4] A.Q. da Silva, D.M. de Souza Abessa, Toxicity of three emerging contaminants to non-target marine organisms, Environ. - Ment. Sci. Pollut. Res. 26 (2019) 18354–18364, https://doi.org/10.1007/s11356-019-05151-9.

[5] M. del Carmen Ramírez-Montero, L.M. Gómez-Oliván, V.M. Gutíerrez-Noya, J. M. Orozco-Hernández, H. Islas-Flores, G.A. Elizalde-Velázquez, N. SanJuan-Reyes, M. Galar-Martínez, Acute exposure to 17α-ethinylestradiol disrupt the embryonic development and oxidative status of Danio rerio, Comp. Biochem. Physiol. Part C: Toxicol. Pharmacol. 251 (2022), 109199, https://doi.org/10.1016/j.cbpc.2021.109199.

[6] B.O. Orimolade, O.A. Arotiba, Enhanced photoelectrocatalytic degradation of diclofenac sodium using a system of Ag $BiVO_4$/BiOI anode and Ag BiOI cathode, Sci. Rep. 12 (2022) 4214, https://doi.org/10.1038/s41598-022-08213-0.

[7] M. Shaban, A.M. Ashraf, M.R. Abukhadra, TiO_2 nanoribbons/carbon nanotubes composite with enhanced photocatalytic activity; fabrication, characterization, and application, Sci. Rep. 8 (1) (2018) 1–17, https://doi.org/10.1038/s41598-018-19172-w.

[8] P.V.G. Reddy, B.R.P. Reddy, M.V.K. Reddy, K.R. Reddy, N.P. Shetty, T.A. Saleh, T. M. Aminabhavi, A review on multicomponent reactions catalysed by zero-dimensional/one-dimensional titanium dioxide (TiO_2) nanomaterials: promising green methodologies in organic chemistry, J. Environ. Manag. 279 (2021), 111603, https://doi.org/10.1016/j.jenvman.2020.111603.

[9] A. Petala, Z. Frontistis, M. Antonopoulou, I. Konstantinou, D.I. Kondarides, D. Mantzavinos, Kinetics of ethyl paraben degradation by simulated solar radiation in the presence of n-doped TiO_2 catalysts, Water Res. 81 (2015) 157–166, https://doi.org/10.1016/j.watres.2015.05.056.

[10] H.G. Oliveira, L.H. Ferreira, R. Bertazzoli, C. Longo, Remediation of 17α-ethinylestradiol aqueous solution by photocatalysis and electrochemically-assisted photocatalysis using TiO_2 and TiO_2/WO_3 electrodes irradiated by a solar simulator, Water Res. 72 (2015) 305–314, https://doi.org/10.1016/j.watres.2014.08.042 (occurrence, fate, removal and assessment of emerging contaminants in water in the water cycle (from wastewater to drinking water)).

[11] S. Giannakopoulos, Z. Frontistis, J. Vakros, S.G. Poulopoulos, I.D. Manariotis, D. Mantzavinos, Combined activation of persulfate by biochars and artificial light for the degradation of sulfamethoxazole in aqueous matrices, J. Taiwan Inst. Chem. Eng. 136 (2022), 104440, https://doi.org/10.1016/j.jtice.2022.104440.

[12] F. Zhu, J. Ma, Q. Ji, H. Cheng, S. Komarneni, Visible-light-driven activation of sodium persulfate for accelerating orange II degradation using $ZnMn_2O_4$ photocatalyst, Chemosphere 278 (2021), 130404, https://doi.org/10.1016/j.chemosphere.2021.130404.

[13] K. Lalas, O.S. Arvaniti, E. Zkeri, M.-C. Nika, N.S. Thomaidis, D. Mantzavinos, A. S. Stasinakis, Z. Frontistis, Thermally activated persulfate oxidation of ampicillin: kinetics, transformation products and ecotoxicity, Sci. Total Environ. 846 (2022), 157378, https://doi.org/10.1016/j.scitotenv.2022.157378.

[14] A. Ioannidi, O.S. Arvaniti, M.-C. Nika, R. Aalizadeh, N.S. Thomaidis, D. Mantzavinos, Z. Frontistis, Removal of drug losartan in environmen- tal aquatic matrices by heat-activated persulfate: kinetics, transforma- tion products and synergistic effects, Chemosphere 287 (2022), 131952, https://doi.org/10.1016/j.chemosphere.2021.131952.

[15] O.S. Arvaniti, F. Bairamis, I. Konstantinou, D. Mantzavinos, Z. Frontis- tis, degradation of antihypertensive drug valsartan in water matrices by heat and heat/ultrasound activated persulfate: kinetics, synergy effect and transformation products, Chem. Eng. J. Adv. 4 (2020), 100062, https://doi.org/10.1016/j.ceja.2020.100062.

[16] E. Avramiotis, Z. Frontistis, I.D. Manariotis, J. Vakros, D. Mantzavinos, On the performance of a sustainable rice husk biochar for the activation of persulfate and the degradation of antibiotics, Catalysts 11 (11) (2021), https://doi.org/10.3390/catal11111303.

[17] V. Matthaiou, Z. Frontistis, A. Petala, M. Solakidou, Y. Deligiannakis, G. N. Angelopoulos, D. Mantzavinos, Utilization of raw red mud as a source of iron activating the persulfate oxidation of paraben, Process Saf. Environ. Prot. 119 (2018) 311–319, https://doi.org/10.1016/j.psep.2018.08.020.

[18] Z. Frontistis, Degradation of the nonsteroidal anti-inflammatory drug piroxicam from environmental matrices with UV-activated persulfate, J. Photochem. Photobiol. A Chem. 378 (2019) 17–23, https://doi.org/10.3390/ijerph15112600.

[19] A. Cordova, Q. Peng, I.L. Ferrall, A.J. Rieth, P.G. Hoertz, J.T. Glass, Enhanced photoelectrochemical water oxidation via atomic layer deposition of TiO_2 on fluorine-doped tin oxide nanoparticle films, Nanoscale 7 (2015) 8584–8592, https://doi.org/10.1039/C4NR07377K.

[20] I.A. Castro, G. Byzynski, M. Dawson, C. Ribeiro, Charge transfer mechanism of WO_3/TiO_2 heterostructure for photoelectrochemical water splitting, J. Photochem. Photobiol. A Chem. 339 (2017) 95–102, https://doi.org/10.1016/j.jphotochem.2017.02.024.

[21] J. Wang, T. Zhou, Y. Zhang, S. Chen, J. Bai, J. Li, H. Zhu, B. Zhou, The design of high performance photoanode of CQDs/TiO_2/WO_3 based on DFT alignment of lattice parameter and energy band, and charge distribution, J. Colloid Interface Sci. 600 (2021) 828–837, https://doi.org/10.1016/j.jcis.2021.05.086.

[22] Y. Liu, X. Yan, Z. Kang, Y. Li, Y. Shen, Y. Sun, L. Wang, Y. Zhang, Synergistic effect of surface plasmonic particles and surface passivation layer on ZnO nanorods array for improved photoelectrochemical water splitting, Sci. Rep. 6 (2016) 1–7, 2016 61, ⟨https://ui.adsabs.harvard.edu/link_gateway/2016NatSR.629907L/doi:10.1038/srep29907⟩.

[23] M. Long, D. Li, H. Li, X. Ma, Q. Zhao, Q. Wen, F. Song, Synergetic effect of photocatalysis and peroxymonosulfate activated by MFe2O4 (M = Co, Mn, or Zn) for enhanced photocatalytic activity under visible light irradiation, RSC Adv. 32 (2022), https://doi.org/10.1039/D2RA03558H.

[24] A. Petala, G. Bampos, Z. Frontistis, Using sawdust derived biochar as a novel 3D particle electrode for micropollutants degradation, Water 14 (3) (2022), https://doi.org/10.3390/w14030357.

[25] B.O. Orimolade, A.O. Idris, U. Feleni, B. Mamba, Peroxymonosulfate assisted photoelectrocatalytic degradation of phar maceuticals at a FTO Bi_2WO_6 electrode: mechanism and kinetics studies, Catal. Commun. 169 (2022), 106481, https://doi.org/10.1016/j.catcom.2022.106481.

[26] H. Shao, Y. Wang, H. Zeng, J. Zhang, Y. Wang, M. Sillanpää, X. Zhao, Enhanced photoelectrocatalytic degradation of Bisphenol A by $BiVO_4$ photoanode coupling with peroxymonosulfate, J. Hazard. Mater. 394 (2020), 121105, https://doi.org/10.1016/j.jhazmat.2019.121105.

[27] R.M. Aleisa, H. Duan, J. Zhang, Y. Yin, M. Xing, Metallic active sites on MoO_2(110) surface to catalyze advanced oxidation processes for efficient pollutant removal, iScience 23 (2020), https://doi.org/10.1016/j.isci.2020.100861.

[28] W. Ren, C. Cheng, P. Shao, X. Luo, H. Zhang, S. Wang, X. Duan, Origins of electron-transfer regime in persulfate-based nonradical oxidation processes, Environ. Sci. Technol. 56 (2022) 78–97, https://doi.org/10.1021/acs.est.1c05374.

[29] Y. Yang, P. Zhang, K. Hu, P. Zhou, Y. Wang, A.H. Asif, X. Duan, H. Sun, S. Wang, Crystallinity and valence states of manganese oxides in Fenton-like polymerization of phenolic pollutants for carbon recycling against degradation, Appl. Catal. B: Environ. 315 (2022), https://doi.org/10.1016/j.apcatb.2022.121593.

[30] J.D. García-Espinoza, P. Mijaylova-Nacheva, M. Avilés-Flores, Electrochemical carbamazepine degradation: effect of the generated active chlorine, transformation pathways and toxicity, Chemosphere 192 (2018) 142–151, https://doi.org/10.1016/j.chemosphere.2017.10.147.

[31] N. Pueyo, M.P. Ormad, N. Miguel, P. Kokkinos, A. Ioannidi, D. Mantzavinos, Z. Frontistis, Electrochemical oxidation of butyl paraben on boron doped diamond in environmental matrices and comparison with sulfate radical-AOP, J. Environ. Manag. 269 (2020), 110783, https://doi.org/10.1016/j.jenvman.2020.110783.

[32] M. Krivec, R. Dillert, D.W. Bahnemann, A. Mehle, J. Štrancar, G. Dražić, The nature of chlorine-inhibition of photocatalytic degradation of dichloroacetic acid in a TiO_2-based microreactor, Phys. Chem. Chem. Phys. 16 (28) (2014) 14867–14873, https://doi.org/10.1039/c4cp01043d.

[33] R. Bruninghoff, A.K. Van Duijne, L. Braakhuis, P. Saha, A.W. Jeremiasse, B. Mei, G. Mul, Comparative analysis of photocatalytic and electrochemical degradation of 4-ethylphenol in saline conditions, Environ. Sci. Technol. 53 (15) (2019) 8725–8735, https://doi.org/10.1021/acs.est.9b01244.

[34] L. Mais, S. Palmas, M. Mascia, A. Vacca, Effect of potential and chlorides on photoelectrochemical removal of diethyl phthalate from water, Catalysts 11 (8) (2021), https://doi.org/10.3390/catal11080882.

[35] W. Zhang, T. An, M. Cui, G. Sheng, J. Fu, Effects of anions on the photocatalytic and photoelectrocatalytic degradation of the reactive dye in a packed-bed reactor, J. Chem. Technol. Biotechnol., 80, pp. 223–229. ⟨https://doi.org/10.1002/jctb.1185⟩.

[36] L. Chen, C. Lei, Z. Li, B. Yang, X. Zhang, L. Lei, Electrochemical activation of sulfate by BDD anode in basic medium for efficient removal of organic pollutants, Chemosphere 210 (2018) 516–523, https://doi.org/10.1016/j.chemosphere.2018.07.043.

[37] R. Montenegro-Ayo, J.C. Morales-Gomero, H. Alarcon, S. Cotillas, P. Westerhoff, S. Garcia-Segura, Scaling up photoelectrocatalytic reactors: a TiO_2 nanotube-coated disc compound reactor effectively degrades acetaminophen, Water 11 (12) (2019), https://doi.org/10.3390/w11122522.

[38] H. Lebik-Elhadi, Z. Frontistis, H. Ait-Amar, S. Amrani, D. Mantzavinos, Electrochemical oxidation of pesticide thiamethoxam on boron doped diamond anode: role of operating parameters and matrix effect, Process Saf. Environ. Prot. 116 (2018) 535–541, https://doi.org/10.1016/j.psep.2018.03.021.